Carbohydrate Research 345 (2010) 1958–1962

Contents lists available at ScienceDirect

Carbohydrate Research

journal homepage: www.elsevier.com/locate/carres

Note

Cloning and in vitro characterization of dTDP-6-deoxy-L-talose biosynthetic genes from *Kitasatospora kifunensis* featuring the dTDP-6-deoxy-L-*lyxo*-4-hexulose reductase that synthesizes dTDP-6-deoxy-L-talose

Suman Karki, Hye-Gyeong Yoo, So-Yeon Kwon, Joo-Won Suh, Hyung-Jin Kwon *

Department of Biological Science, Division of Bioscience and Bioinformatics, Myongji University, Yongin 449-728, Republic of Korea

ARTICLE INFO

Article history:
Received 11 May 2010
Received in revised form 25 June 2010
Accepted 4 July 2010

Keywords:
dTDP-6-Deoxy-L-talose
Kitastospora kifunensis
Biosynthetic gene cluster
dTDP-6-Deoxy-L-*lyxo*-4-hexulose reductase

ABSTRACT

Kitasatospora kifunensis, the talosin producer, was used as a source for the dTDP-6-deoxy-L-talose (dTDP-6dTal) biosynthetic gene cluster, serving as a template for four recombinant proteins of $RmlA_{Kkf}$, $RmlB_{Kkf}$, $RmlC_{Kkf}$, and Tal, which complete the biosynthesis of dTDP-6dTal from dTTP, α-D-glucose-1-phosphate, and NAD(P)H. The identity of dTDP-6dTal was validated using ^{1}H and ^{13}C NMR spectroscopy. *K. kifunensis tal* and *tll*, the known dTDP-6dTal synthase gene of *Actinobacillus actinomycetemcomitans* origin, have low sequence similarity and are distantly related within the NDP-6-deoxy-4-ketohexose reductase family, providing an example of the genetic diversity within the dTDP-6dTal biosynthetic pathway.

6-Deoxyhexoses are well-known components of cell surface glycans and secondary metabolites in bacteria.[1,2] 6-Deoxyhexoses are biosynthesized in the form of nucleotide diphosphate (NDP)-6-deoxyhexoses, exemplified in the biosynthesis of thymidine diphosphate (dTDP)-L-rhamnose. dTDP-L-rhamnose (dTDP-Rha) is synthesized through a series of reactions involving glucose-1-phosphate thymidylyltransferase (RmlA), dTDP-D-glucose 4,6-dehydratase (RmlB), dTDP-6-deoxy-D-*xylo*-4-hexulose 3,5-epimerase (RmlC), and dTDP-6-deoxy-L-*lyxo*-4-hexulose reductase (RmlD) (Fig. 1). The committed step in the synthesis of dTDP-6-deoxyhexose pathway is the RmlB reaction, and diverse dTDP-6-deoxyhexose structures are generated by enzymatic modifications of the product of this reaction, dTDP-6-deoxy-D-*xylo*-4-hexulose.[3]

6-Deoxy-L-talose (6dTal) is a component of the bacterial lipopolysaccharides and capsular polysaccharides. Based on similarity to the dTDP-Rha pathway, the dTDP-6dTal pathway was hypothesized to involve either dTDP-Rha 4-epimerase activity or dTDP-6-deoxy-L-*lyxo*-4-hexulose reductase activity with a stereospecificity that opposes that of RmlD (Fig. 1). Early cell-free experiments in *Escherichia coli* O45 demonstrated that a pair of stereospecific 4-keto-reductions led to the formation of dTDP-Rha and dTDP-6dTal.[4] The O-antigenic polysaccharide (O-PS) moieties of lipopolysaccharides from *E. coli* and *Burkholderia pseudomallei* contain 6dTal[5,6] and the cognate biosynthetic gene cluster of *B. pseudomallei* was found to encode three nucleotide sugar 4-epimerases in addition to RmlABCD.[7] It was proposed that one of these epimerases synthesizes dTDP-6dTal from dTDP-Rha.

Capsular polysaccharides of *Actinobacillus actinomycetemcomitans* serotype c contain 6-deoxy-L-talan, the 6dTal polymer, whereas 6-deoxy-D-talan is found in serotype a.[8] 6-Deoxy-L-talan has also been characterized in lipopolysaccharides of *Rhizobium loti*[9] and capsular polysaccharides of *Agrobacterium rubi*.[10] Cloning of the 6-deoxy-L-talan biosynthetic gene cluster from *A. actinomycetemcomitans* and its subsequent biochemical characterization revealed that dTDP-Rha and dTDP-6dTal are synthesized through stereospecific 4-keto-reductions of dTDP-6-deoxy-L-*lyxo*-4-hexulose mediated by RmlD and Tll, respectively (Fig. 1).[11–13] 6dTal is also found in the surface glycopeptidolipid of *Mycobacterium avium* and other *Mycobacterium* strains.[14,15] However, a homology search failed to reveal a *tll* ortholog from genomes of these strains, which implies genetic diversity within the bacterial dTDP-6dTal biosynthetic pathway. We cloned and characterized the dTDP-6dTal biosynthetic genes from *Kitasatospora kifunensis*, a rare actinomycetes, to investigate the genetic diversity within this pathway.

K. kifunensis produces talosins, the genistein glycosides of 6dTal.[16] It has been proposed that talosin is produced from exogenous genistein in soybean meal, which is included in fermentation medium, and that *K. kifunensis* has the potential to generate dTDP-6dTal. Through PCR targeted to *rmlB*, we were able to clone a 9605 bp region surrounding this gene from *K. kifunenesis* (Fig. 2). There are 11 predicted ORFs within this region, including $rmlA_{Kkf}$, $rmlB_{Kkf}$, and $rmlC_{Kkf}$ (ORF5, 6, and 7, respectively). The products of ORF5, 6, and 7 show 76%, 62%, and 66% similarities, respectively,

* Corresponding author. Tel.: +82 31 330 6470; fax: +82 31 335 8249.
E-mail address: hjink@mju.ac.kr (H.-J. Kwon).

0008-6215/$ - see front matter © 2010 Elsevier Ltd. All rights reserved.
doi:10.1016/j.carres.2010.07.004

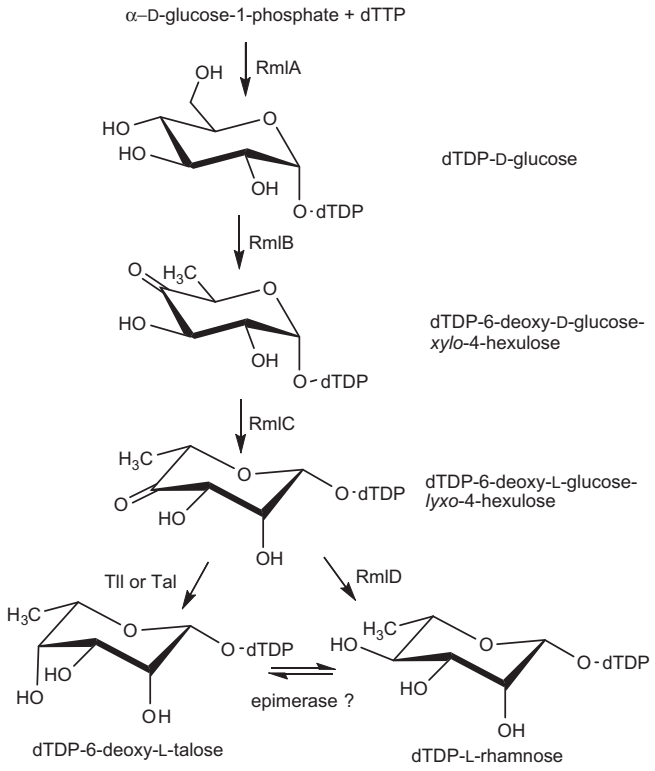

Figure 1. Biosynthetic pathways of both dTDP-L-rhamnose and dTDP-6-deoxy-L-talose (dTDP-6dTal). The formation of dTDP-6dTal by Tll reductase was previously described[12] while the Tal-mediated formation of dTDP-6dTal was validated in this study. The epimerization reaction is speculative and lacks experimental support.

to the dTDP-Rha biosynthetic enzymes of *Mycobacterium tuberculosis* H37Rv. In addition, this region contains ORFs for glycosyltransferases (ORF1, ORF8, and ORF11, which is N-terminally truncated), an NDP-hexose 4-ketoreductase (ORF9), an O-antigen acetyltransferase (ORF10), and four hypothetical proteins. The product of ORF9 (named *tal*) is similar (percentage similarity, amino acids that overlap) to the NDP-4-keto-6-deoxyhexose reductases of *Streptomyces*, including those of *med*-ORF14 (57%, 317),[17] *hedN* (57%, 297),[18] and *dnmV* (50%, 314),[19] while showing low similarity to Tll (37%, 265) and RmlD proteins (37%, 222, with StrL from *Streptomyces griseus*). The predicted functions of Med-ORF14 and HedN are dTDP-3-amino-4-keto-2,3,6-trideoxy-D-glucose 4-ketoreductase in the biosynthesis of dTDP-D-angolosamine.[17,18] DnmV is dTDP-3-amino-4-keto-2,3,6-trideoxy-L-glucose 4-ketoreductase in dTDP-L-daunosamine biosynthesis.[19] Notably, these enzymes display the same stereospecificity as Tll in the 4-keto-reduction although their substrates differ in D- and L-configurations. ORF10 is homologous to *wbiA* (53%, 346), which is a member of the O-PS biosynthetic gene cluster from *B. pseudomallei*.[7] The *wbiA* locus was shown to be responsible for the acetylation of the 6-deoxy-L-talosyl residue at O-2 position in O-PS of *B. pseudomallei*.[20] Overall, the homology analysis suggests that the region we cloned belongs to the biosynthetic gene cluster of the extracellular glycan that contains 6dTal or Rha.

To examine whether $RmlA_{Kkf}$, $RmlB_{Kkf}$, $RmlC_{Kkf}$, and Tal constitute the dTDP-6dTal biosynthetic pathway, these proteins were over-expressed and purified as hexa-histidine fusions (Supplementary data). When $RmlA_{Kkf}$ was incubated with 1 mM thymidine triphophate (dTTP) and 5 mM α-D-glucose-1-phosphate, dTTP was quantitatively converted into a new compound, which we assigned as dTDP-D-glucose (Fig. 3a and b). When $RmlB_{Kkf}$ was added to the $RmlA_{Kkf}$ reaction mixture, the dTDP-D-glucose peak was reduced and a new broad peak was observed (Fig. 3c). In the HPLC conditions used, dTDP-4-keto-6-deoxy-D-glucose produces a broad peak,[12] suggesting that the $RmlA_{Kkf}$/$RmlB_{Kkf}$ reaction successfully generated dTDP-4-keto-6-deoxy-D-glucose. When $RmlC_{Kkf}$ and Tal were added to the $RmlA_{Kkf}$/$RmlB_{Kkf}$ reaction mixture together with either nicotinamide adenine dinucleotide or nicotinamide adenine dinucleotide phosphate, the formation of a new product was observed at 50 min in both cases (Fig. 3d and e). We determined the structure of this product using NMR spectroscopy.

Ten milliliters of the $RmlA_{Kkf}$/$RmlB_{Kkf}$/$RmlB_{Kkf}$/Tal reaction sample were processed by HPLC and subsequently used for NMR measurements (Fig. 4). The ^1H and ^{13}C NMR spectral assignments are presented in Table 1. The ^1H NMR data are in good agreement with the previously reported data of dTDP-6-dTal,[12] indicating that Tal has the same catalytic role as Tll (Table 1). Small coupling constants for H-3″ and H-4″ splitting, which were calculated as ~3.0 and 3.1 Hz, respectively, are indicative of dTDP-6dTal. H-6″ appears to be correlated with H-4″ and H-5″ in the NOESY spectra,

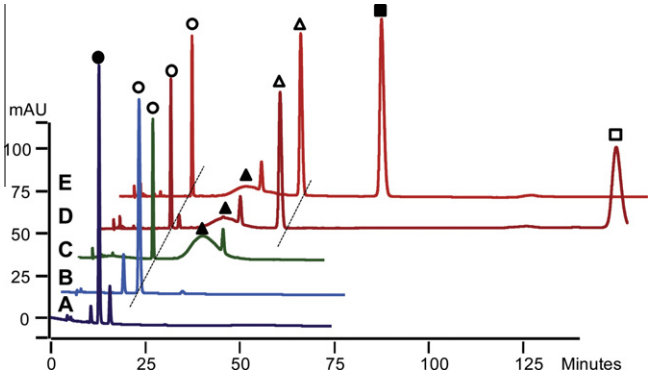

Figure 3. HPLC profiles of the enzyme reactions for dTDP-6-deoxy-L-talose synthesis. A: authentic dTTP. B: $RmlA_{Kkf}$ with dTTP and α-D-glucose-1-phosphate. C: $RmlA_{Kkf}$ and $RmlB_{Kkf}$ with dTTP and α-D-glucose-1-phosphate. D: $RmlA_{Kkf}$, $RmlB_{Kkf}$, $RmlC_{Kkf}$, and Tal with dTTP, α-D-glucose-1-phosphate, and NADH. E: $RmlA_{Kkf}$, $RmlB_{Kkf}$, $RmlC_{Kkf}$, and Tal with dTTP, α-D-glucose-1-phosphate, and NADPH. A closed circle: dTTP, open circles: dTDP-D-glucose, closed triangles: dTDP-4-keto-6-deoxy-D-glucose, open triangles: dTDP-6-deoxy-L-talose, an open rectangle: NAD^+, a closed rectangle: $NADP^+$.

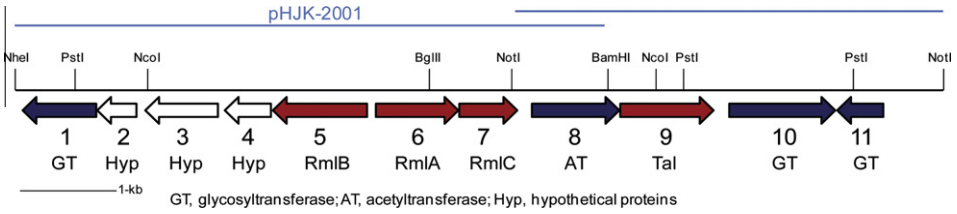

Figure 2. Restriction map and gene organization of the 9605-bp DNA region isolated from *Kitasatospora kifunensis*. Coverage of the two sequenced plasmid clones is shown. Deduced function of each gene product is provided below the map.

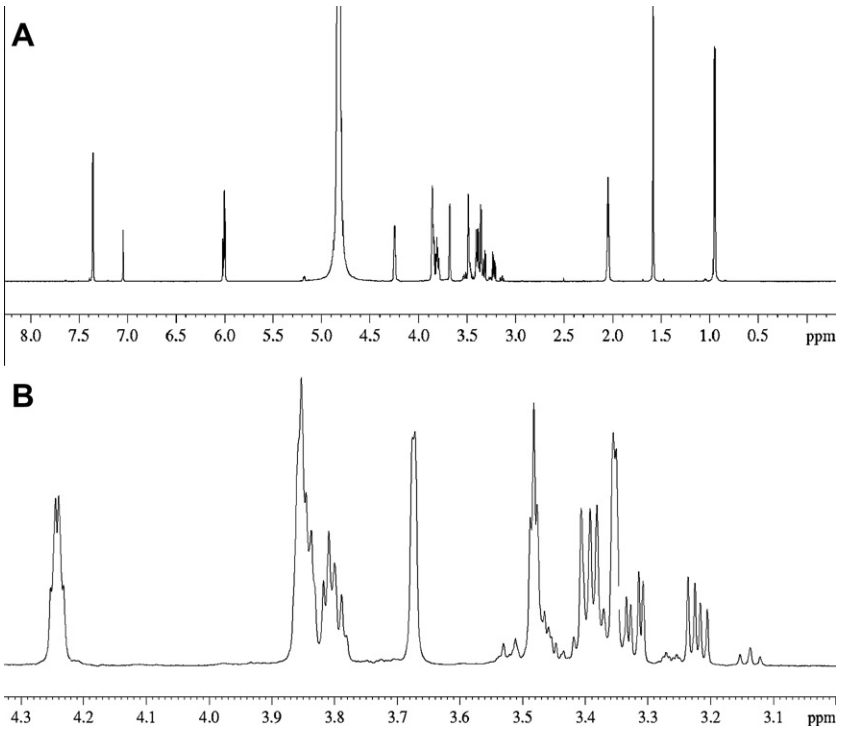

Figure 4. ^{1}H NMR spectra of dTDP-6-deoxy-L-talose from the $RmlA_{Kkf}$/$RmlB_{Kkf}$/$RmlC_{Kkf}$/Tal reaction in the presence of dTTP, α-D-glucose-1-phosphate, and NADH. (A) The spectra were obtained in pure D_2O. Panel B is an expansion of the H-2″–H-5″ region.

further supporting the identity of dTDP-6dTal (Supplementary data).

In conclusion, Tal performs the same chemical reaction as Tll in the biosynthesis of dTDP-6dTal despite the fact that these proteins share a low similarity. We speculate that Tal and Tll took separate evolutionary tracks that functionally converged. Phylogenetic analysis supports the idea that Tal and Tll belong to discrete phylogenetic clades (Fig. 5). The absence of a *tll* homolog in the O-PS biosynthetic gene cluster from *B. pseudomallei*[7] led to the proposal that *B. pseudomallei* synthesizes dTDP-6dTal through C″-4 epimerization of dTDP-Rha, while *A. actinomycetemcomitans* utilizes Tll activity for that purpose.[12] Although any of the three putative epimerases (WbiB, WbiG, or WbiI) predicted in the O-PS biosynthetic gene cluster does not show a strong homology to Tal, phylogenetic analysis indicates that these putative epimerases are more closely related to Tal than UDP-D-glucose 4-epimerases (data not shown). Our results highlight a possibility that the dTDP-6-deoxy-L-*lyxo*-4-hexulose reductase gene involved in the biosynthesis of dTDP-6dTal is encoded in the O-PS biosynthetic gene cluster of *B. pseudomallei.* As such, our results provide new insight into the analysis of the glycan biosynthetic genes of bacterial genomes.

1. Experimental

1.1. Bacterial strains

K. kifunensis MJM341 was a provision of Extract Collection of Useful Microorganisms (ECUM) at Myongji University, Yongin, Korea. *K. kifunensis* was maintained in Bennett agar and cultured in TSB (10 mM $MgCl_2$, 0.5% glycine) for total DNA isolation. *E. coli* DH5α was used for general subcloning.

1.2. Gene cloning procedures

Degenerate PCR primers were used to clone an internal fragment of *rmlB* from *K. kifunenesis*. The primer pairs are: 5′-CSGGSGSSGCSGGSTTCATCGG-3′ (forward) and 5′-GGGWRCTGGYRSGGSCCSTAGTTG-3′ (reverse).[22] A distinct product of the predicted size (0.55 kb) was amplified and cloned into pGEM-T vector. The *rmlB* fragment was used as a probe in Southern blot experiment with *K. kifunensis* genomic DNA which was di-

Table 1
NMR spectroscopy identification of dTDP-6-deoxy-L-talose from the RmlA/RmlB/RmlC/Tal reaction

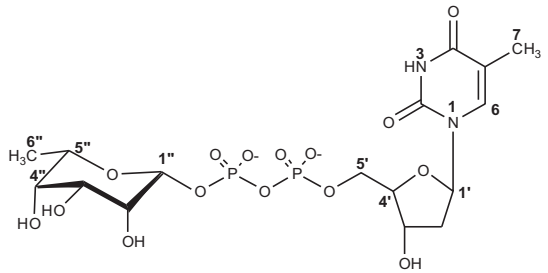

Atom	δ_c	δ_H (number of H, splitting[a], *J*)
2	153.5	
4	168.2	
5	113.4	
6	139.0	7.71 (1H, s)
7	13.5	1.93 (3H, s)
1′	86.6	6.35 (1H, m, J_d = 6.7)
2′	40.2	2.38 (2H, m, J_d = 5.8)
3′	72.6	4.60 (1H, m)
4′	86.7	4.19 (1H, m)
5′	67.4	4.19 (1H, m), 4.15 (1H, m)
1″	97.7	5.14 (1H, d, *J* = 8.8)
2″	71.8	4.02 (1H, d, *J* = 2.5)
3″	69.8	3.82 (1H, dd, J_1 = ∼3.0, J_2 = ∼3.0)
4″	72.0	3.68 (1H, d, *J* = 3.1)
5″	74.0	3.74 (1H, m, J_1[b] = ∼6.4)
6″	17.3	1.29 (3H, d, *J* = 6.5)

[a] Observed splitting pattern.
[b] Coupling constant for quartet.

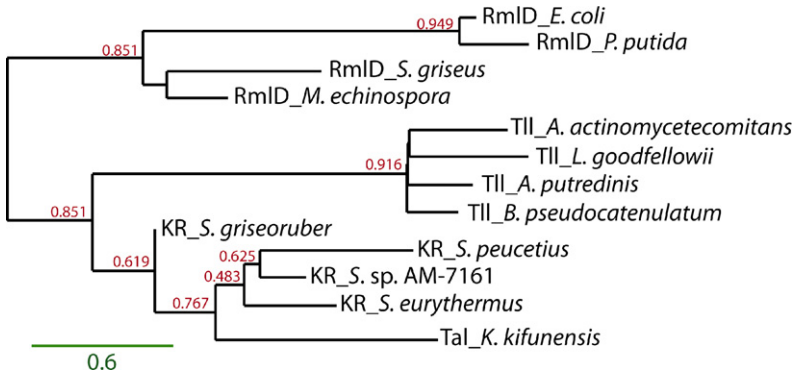

Protein	Amino acids	Source organism	Sequence source	GenBank accession number no.
RmlD_*E. coli*	299	*Escherichia coli*	Biochemically characterized	ADB02812
RmlD_*P. putida*	301	*Pseudomonas putida*	Genome search	ABY97288
RmlD_*S. griseus*	304	*Streptomyces griseus*	Streptomycin biosynthetic gene cluster (*strL*), function predicted	CAA44443
RmlD_*M. echinospora*	307	*Micromonospora echinospora*	Calicheamicin biosynthetic gene cluster (*calS2*), function predicted	AAM94769
Tll_*A. actinomycetecomitans*	270	*Actinobacillus actinomycetecomitans*	6-Deoxy-L-talan biosynthetic gene cluster[11,12]	BAA28138
Tll_*L. goodfellowii*	279	*Leptotrichia goodfellowii*	Genome search	EEY35364
Tll_*A. putredinis*	279	*Alistipes putredinis*	Genome search	EDS02198
Tll_*B. pseudocatenulatum*	288	*Bifidobacterium pseudocatenulatum*	Genome search	EEG70112
KR_*S. griaeoruber*	321	*Streptomyces griaeoruber*	Hedamycin biosynthetic gene cluster (*hedN*), function predicted[18]	AAP85346
KR_*S. peucetius*	307	*Streptomyces peucetius*	Daunorubicin biosynthetic gene cluster (*dnmV*), genetic evidence[19]	AAB63047
KR_*S.* sp. AM-7161	325	*Streptomyces* sp. AM-7161	Medermycin biosynthetic gene cluster (*med-orf14*), function predicted[17]	BAC79033
KR_*S. erythermus*	333	*Streptomyces erythermus*	Unknown polyketide biosynthetic gene cluster	ABV49596
Tal_*K. kifunensis*	318	*Kitasatospora kifunensis*	This study	HM132058

Figure 5. Phylogenetic analysis of NDP-4-keto-6-deoxyhexose reductase proteins (including Tll and Tal). Branch length is proportional to the number of substitutions per site. The branch support values are shown. Identities of the proteins are given in the table below. Phylogenetic tree was generated in the Phylogeny.fr platform.[21] The phylogenetic tree was reconstructed using the maximum likelihood method implemented in the PHYML program (v3.0 aLRT).

gested with BamHI and NheI. The Southern blot gave rise to a hybridization signal at 6-kb region in agarose gel separation. The 6-kb region was purified and used to construct a mini-library in pGEM-11zf. Three hundred colonies were screened with colony blot analysis, giving rise to pHJK-2001. A 4.6 kb NotI fragment, which overlapped with the 6-kb BamHI/NheI fragment, was also isolated through genomic Southern blot and cloned into pBluescript-SK, giving rise to pHJK-2002. pHJK-2001 and pHJK-2002 were sequenced and the resulting sequence was deposited in GenBank (http://www.ncbi.nlm.nih.gov/Genbank) under the accession number HM132058. Southern hybridization was performed with the digoxigenin-labeled DNA following the manufacturer's procedure (Roche Diagnostics, Pleasanton, CA).

1.3. Protein expression and purification

PCR amplification was used to prepare the expression constructs. The PCR primers (with engineered NdeI and HindIII sites underlined) are 5′-attcatATGCGTGGAATCCTCTTGGCC-3′ and 5′-attaagcttTCACTTGGCCGCCTCCTC-3′ (*rmlA*$_{Kkf}$), 5′-attcatATGCGCATCCTCGTCACCGGC-3′ and 5′-attaagcttTCATCGCAGCGCGGCCTT-3′ (*rmlB*$_{Kkf}$), 5′-attcatATGAAGTTCCGCGAACTGTCC-3′ and 5′-attaagcttTCAGTTGGTGCGCAGGCC-3′ (*rmlC*$_{Kkf}$), 5′-attcatATGACCGCTCCGCACACGGCA-3′ and 5′-attaagcttTTATGCGACCGGCGCGGT-3′ (*tal*). PCR products were digested with NdeI and HindIII and cloned into the same sites of pUC18. From the resulting plasmids, the inserts were recovered as NdeI and HindIII fragments and ligated into pET-28b, giving rise to pHJK-2011 (*rmlA*$_{Kkf}$), pHJK-2012 (*rmlB*$_{Kkf}$), pHJK-2013 (*rmlC*$_{Kkf}$), and pHJK-2014 (*tal*). Each plasmid was transformed into *E. coli* BL21 (DE3). Overnight cultures were used to inoculate 50 mL of LB medium supplemented with 50 μg/mL kanamycin. The cultures were grown at 37 °C until they reached an OD_{600}-reading of 0.6. The cultures were then induced with 1 mM IPTG and grown for an additional 4 h at 28 °C (for *rmlA*$_{Kkf}$ and *rmlB*$_{Kkf}$) or 37 °C (for *rmlC*$_{Kkf}$ and *tal*). The 6xhistidine-tagged proteins were isolated using a Ni-NTA agarose resin, following the

manufacturer's protocol (Qiagen, Valencia, CA). The protein content was determined using the Bradford assay. Purified protein yields were 11 ($RmlA_{Kkf}$), 1.0 ($RmlB_{Kkf}$), 747 ($RmlC_{Kkf}$), and 16 (Tal) mg/L from the culture. For the recombinant $RmlB_{Kkf}$, 500 mL LB culture was further processed to obtain 1 mg of protein. The concentrations of the protein solutions were 32 ($RmlA_{Kkf}$), 54 ($RmlB_{Kkf}$), 150 ($RmlC_{Kkf}$), and 49 (Tal) μM.

1.4. Enzyme reaction

The formation of dTDP-6dTal was monitored in a two-step, one-pot reaction with recombinant $RmlA_{Kkf}$, $RmlB_{Kkf}$, $RmlC_{Kkf}$, and Tal proteins. $RmlA_{Kkf}$/$RmlB_{Kkf}$ reaction mixture contained 1 mM thymidine triphosphate (dTTP), 5 mM α-D-glucose-1-phosphate, 10 mM $MgCl_2$, 50 mM KH_2PO_4 (pH 7.5), 0.8 μM $RmlA_{Kkf}$, 1.4 μM $RmlB_{Kkf}$, and 1 U/mL pyrophosphatase (Sigma). The reaction mixture was incubated at 37 °C for 14–20 h. Five millimolar nicotinamide adenine dinucleotide (NAD), 3.75 μM $RmlC_{Kkf}$, and 1.2 μM Tal were added to the resulting mixture and incubated at 37 °C for 2 h. The formation of dTDP-6dTal was monitored using HPLC as previously described.[12] Separation was performed in an ODS-A column (250 × 10 mm; YMC, Kyoto, Japan) with 0.5 M KH_2PO_4 as the mobile phase and a flow rate of 3.0 mL/min. The UV absorbance of the elution was monitored at 264 nm.

1.5. Purification of dTDP-6-deoxy-L-talose and NMR spectroscopy

dTDP-6-Deoxy-L-talose collected by HPLC was used for NMR analysis. The reaction mixture was loaded on an HPLC column after ultrafiltration (molecular weight cut-off of 30,000 kDa). The HPLC elution was lyophilized after removal of the excess phosphate as previously described.[12] The fraction from each run was cooled on ice and pooled with four volumes of cold ethanol to remove the excess phosphate. The ethanol solution was dried under reduced pressure and dissolved in one tenth volumes of water to be lyophilized. NMR experiments such as ^1H NMR, ^{13}C NMR, ^1H–^1H COSY, NOESY, ^1H–^{13}C HMQC, and ^1H–^{13}C HMBC were conducted in pure D_2O at 23 °C using a Bruker AVANCE 600-MHz spectrometer. ^1H NMR spectra were also recorded with an inclusion of trimethylsilyl propionate to obtain the chemical shift data. The parameters for ^1H NMR spectral recording were as follows: pulse angle, 30°; sweep width, 10776 Hz; acquisition time, 3.04 s; relaxation delay, 1 s; scans number, 64; digital resolution, 0.16 Hz/point.

Acknowledgments

This work was supported by National Research Foundation of Korea Grant funded by the Korean Government (MOEHRD, Basic Research Promotion Fund) (KRF-2008-331-C00244 and 2009-0074283), and a grant (20070401-034023) from the BioGreen 21 Program of the Rural Development Administration, Korea.

Supplementary data

Supplementary data associated with this article can be found, in the online version, at doi:10.1016/j.carres.2010.07.004.

References

1. Mäki, M.; Renkonen, R. *Glycobiology* **2004**, *14*, 1R–15R.
2. Thibodeaux, C. J.; Melançon, C. E.; Liu, H. W. *Angew. Chem., Int. Ed.* **2008**, *47*, 9814–9859.
3. Thibodeaux, C. J.; Melançon, C. E.; Liu, H. W. *Nature* **2007**, *446*, 1008–1016.
4. Gaugler, R. W.; Gabriel, O. *J. Biol. Chem.* **1973**, *248*, 6041–6049.
5. Jann, B.; Shashkov, A.; Torgov, V.; Kochanowski, H.; Seltmann, G.; Jann, K. *Carbohydr. Res.* **1995**, *278*, 155–165.
6. Perry, M. B.; MacLean, L. L.; Schollaardt, T.; Bryan, L. E.; Ho, M. *Infect. Immun.* **1995**, *63*, 3348–3352.
7. DeShazer, D.; Brett, P. J.; Woods, D. E. *Mol. Microbiol.* **1998**, *30*, 1081–1100.
8. Shibuya, N.; Amano, K.; Azuma, J.; Nishihara, T.; Kitamura, Y.; Noguchi, T.; Koga, T. *J. Biol. Chem.* **1991**, *266*, 16318–16323.
9. Russa, R.; Urbanik-Sypniewska, T.; Lindström, K.; Mayer, H. *Arch. Microbiol.* **1995**, *163*, 345–351.
10. De Castro, C.; Gargiulo, V.; Lanzetta, R.; Parrilli, M. *Biomacromolecules* **2007**, *8*, 1047–1051.
11. Nakano, Y.; Yoshida, Y.; Yamashita, Y.; Koga, T. *Biochim. Biophys. Acta.* **1998**, *1442*, 409–414.
12. Nakano, Y.; Suzuki, N.; Yoshida, Y.; Nezu, T.; Yamashita, Y.; Koga, T. *J. Biol. Chem.* **2000**, *275*, 6806–6812.
13. Suzuki, N.; Nakano, Y.; Yoshida, Y.; Nakao, H.; Yamashita, Y.; Koga, T. *Biochim. Biophys. Acta* **2000**, *1517*, 135–138.
14. Chatterjee, D.; Khoo, K. H. *Cell. Mol. Life Sci.* **2001**, *58*, 2018–2042.
15. Fujiwara, N.; Nakata, N.; Maeda, S.; Naka, T.; Doe, M.; Yano, I.; Kobayashi, K. *J. Bacteriol.* **2007**, *189*, 1099–1108.
16. Kim, W. G.; Yoon, T. M.; Kwon, H. J.; Suh, J. W. *J. Antibiot.* **2006**, *59*, 640–645.
17. Ichinose, K.; Ozawa, M.; Itou, K.; Kunieda, K.; Ebizuka, Y. *Microbiology* **2003**, *149*, 1633–1645.
18. Bililign, T.; Hyun, C. G.; Williams, J. S.; Czisny, A. M.; Thorson, J. S. *Chem. Biol.* **2004**, *11*, 959–969.
19. Otten, S. L.; Gallo, M. A.; Madduri, K.; Liu, X.; Hutchinson, C. R. *J. Bacteriol.* **1997**, 4446–4450.
20. Brett, P. J.; Burtnick, M. N.; Woods, D. E. *FEMS Microbiol. Lett.* **2003**, *218*, 323–328.
21. Dereeper, A.; Guignon, V.; Blanc, G.; Audic, S.; Buffet, S.; Chevenet, F.; Dufayard, J. F.; Guindon, S.; Lefort, V.; Lescot, M.; Claverie, J. M.; Gascuel, O. *Nucleic Acids Res.* **2008**, *36*, W465–W469.
22. Liu, W.; Shen, B. *Antimicrob. Agents Chemother.* **2000**, *44*, 382–392.